Development 139, 2594-2603 (2012) doi:10.1242/dev.077891

Maize *multiple archesporial cells 1* (*mac1*), an ortholog of rice *TDL1A*, modulates cell proliferation and identity in early anther development

Chung-Ju Rachel Wang[1,2], Guo-Ling Nan[3], Timothy Kelliher[3], Ljudmilla Timofejeva[1,4], Vanessa Vernoud[5,*], Inna N. Golubovskaya[1,6], Lisa Harper[1,7], Rachel Egger[3], Virginia Walbot[3] and W. Zacheus Cande[1,‡]

SUMMARY

To ensure fertility, complex somatic and germinal cell proliferation and differentiation programs must be executed in flowers. Loss-of-function of the maize *multiple archesporial cells 1* (*mac1*) gene increases the meiotically competent population and ablates specification of somatic wall layers in anthers. We report the cloning of *mac1*, which is the ortholog of rice *TDL1A*. Contrary to prior studies in rice and *Arabidopsis* in which *mac1*-like genes were inferred to act late to suppress trans-differentiation of somatic tapetal cells into meiocytes, we find that *mac1* anthers contain excess archesporial (AR) cells that proliferate at least twofold more rapidly than normal prior to tapetal specification, suggesting that MAC1 regulates cell proliferation. *mac1* transcript is abundant in immature anthers and roots. By immunolocalization, MAC1 protein accumulates preferentially in AR cells with a declining radial gradient that could result from diffusion. By transient expression in onion epidermis, we demonstrate experimentally that MAC1 is secreted, confirming that the predicted signal peptide domain in MAC1 leads to secretion. Insights from cytology and double-mutant studies with *ameiotic1* and *absence of first division1* mutants confirm that MAC1 does not affect meiotic cell fate; it also operates independently of an epidermal, *Ocl4*-dependent pathway that regulates proliferation of subepidermal cells. MAC1 both suppresses excess AR proliferation and is responsible for triggering periclinal division of subepidermal cells. We discuss how MAC1 can coordinate the temporal and spatial pattern of cell proliferation in maize anthers.

KEY WORDS: Anther development, Cell fate acquisition, Plant reproduction, Maize

INTRODUCTION

In animals, primordial germ cells or pluripotent reproductive cells arise during embryo development; however, plant reproductive organs and germ cells differentiate late (Bhatt et al., 2001). During flower development, germ cells arise de novo from sub-epidermal somatic cells (Ma, 2005). In ovules, only a single megaspore mother cell develops and only one of its four meiotic products survives to produce the embryo sac. By contrast, numerous pollen mother cells (PMC) differentiate in anthers, and these undergo meiosis to give rise to tetrads of haploid spores. Although these processes are indispensable for plant sexual reproduction, it remains unclear how germ cells acquire their fates and how sporogenesis is coordinated with somatic development.

A mature maize anther contains four anther lobes each with four somatic layers – epidermis (EP), endothecium (EN), middle layer (ML) and tapetum (TA) – that encircle the PMC (Bedinger and Fowler, 2009). The floral meristem of plants consists of three layers, designated L1, L2 and L3 (Poethig, 1987). Within anther lobes, the L1 differentiates as EP, and the L2 forms the PMC and the inner somatic cell layers (Fig. 1). Analysis of anthers in transverse sections from diverse flowering plants demonstrates a very regular pattern of cell division. Based on this regularity and the absence of cell movement, cell lineage models are proposed to explain development (Kiesselbach, 1949; Ma, 2005; Feng and Dickinson, 2010a). In the classical lineage model, a single L2-derived (L2-d) hypodermal cell in each locule divides periclinally to generate one primary sporogenous cell and one primary parietal (somatic) cell. The latter divides to form a complete layer encircling the sporogenous cell with subsequent periclinal divisions, yielding the three rings of somatic cell types. Centrally, the primary sporogenous cell, also known as an archesporial (AR) cell, proliferates to form a mass of PMCs, and then produces microspores through meiosis.

Detailed confocal microscopic analysis of maize anthers is not consistent with a strict cell lineage model. In anthers smaller than 170 μm, dozens of similar sized L2-d cells beneath the EP in a lobe were arranged in a disorganized manner with no evidence for a hypodermal cell or an early division to separate the somatic and germinal lineages. Then, AR cells arise within a group of ~100 L2-derived somatic cells as enlarged germinal cells (Kelliher and Walbot, 2011). A later step in the lineage model was substantiated by confocal reconstruction: the secondary parietal layer divides periclinally to generate the ML next to the EN, and the TA next to the AR cells.

Recent molecular genetic studies have also addressed plant germ cell fate determination (Feng and Dickinson, 2010a; Ma and Sundaresan, 2010). Several *Arabidopsis thaliana* genes crucial for this process have been isolated and characterized: *SPL/NZZ* (*SPOROCYTELESS/NOZZLE*), *EMS1/EXS* (*EXCESS MALE SPOROCYTES1/EXTRA SPOROGENOUS CELLS*),

[1]Department of Molecular and Cell Biology, University of California, Berkeley, CA 94720, USA. [2]Institute of Plant and Microbial Biology, Academia Sinica, Taipei, 11529 Taiwan. [3]Department of Biology, Stanford University, Stanford, CA 94305, USA. [4]Department of Gene Technology, Tallinn University of Technology, Tallinn 12618, Estonia. [5]Laboratoire de Reproduction et Développement des Plantes, INRA/CNRS/ENS Lyon/Université Lyon 1, F-69364 Lyon, France. [6]N. I. Vavilov Institute of Plant Industry, St Petersburg, 190000, Russia. [7]USDA-ARS Plant Gene Expression Center, Albany, CA 94710, USA.

*Present address: INRA, UMR1347 Agroécologie, BP 86510, F-21000 Dijon, France
‡Author for correspondence (zcande@berkeley.edu)

Accepted 29 April 2012

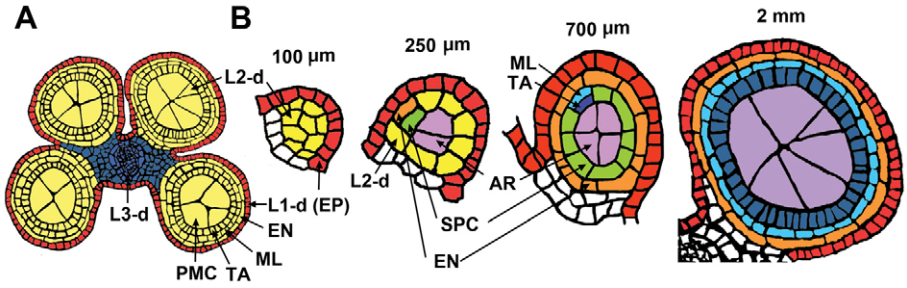

Fig. 1. Anther transverse sections through development. (**A**) An entire 2 mm anther showing all four lobes. The L1-derived (L1-d) cells differentiate into the epidermis (EP, red). The L2-derived (L2-d, yellow) cells differentiate into the somatic endothecium (EN), middle layer (ML), tapetal layer (TA) and the generative pollen mother cells (PMC). The L3-derived (L3-d, blue) cells differentiate into vascular and connective tissue. (**B**) Transverse sections of single lobe from different length anthers. In a 100 μm anther, EP is red and L2-d cells are in yellow. In a 250 μm anther, the archesporial cells (AR, purple) are in the middle of each locule. The L2-d cells start to divide periclinally to form the EN (orange) and secondary parietal cell (SPC) (green). In a 700 μm anther, the SPC (green) starts to divide periclinally to form the TA (dark blue) and the ML (light blue). In a 2 mm anther, all five cell types have developed. The AR cells are called PMCs after they enter meiosis.

TPD1 (*TAPETUM DETERMINANT1*) and *SERK1/2* (*SOMATIC EMBRYO RECEPTOR KINASE 1/2*) (Schiefthaler et al., 1999; Yang et al., 1999; Canales et al., 2002; Zhao et al., 2002; Yang et al., 2003; Albrecht et al., 2005; Colcombet et al., 2005; Yang et al., 2005; Feng and Dickinson, 2010a). *ems1/exs* and *tpd1* mutants and *serk1/serk2* double mutants display the same phenotypes of excess PMCs and absence of the TA (or both TA and ML) (Canales et al., 2002; Zhao et al., 2002; Colcombet et al., 2005; Feng and Dickinson, 2010a). These genes are considered to function in the same pathway to regulate cell fate determination. *EMS1/EXS*, *SERK1* and *SERK2* encode membrane-localized leucine-rich-repeat receptor-like protein kinases (LRR-RLK), and *TPD1* encodes a putative ligand. EMS1/EXS interacts with TPD1 in vitro and in vivo (Yang et al., 2005; Jia et al., 2008). Based on these findings, cell-cell communication has been proposed as essential for anther cell fate determination and differentiation. It has been speculated that SERK1/2 and EMS1/EXS form heterodimeric receptors (Colcombet et al., 2005), but the ability of TPD1 to bind heterodimers is unknown. The precise timing and cellular location of protein expression of the proposed signaling pathway components are also unclear. Nevertheless, two models to explain anther cell specification have been proposed. In the first model, these proteins specify tapetal fate late, after the secondary parietal division produces tapetal precursors; in mutants, those precursors fail to acquire TA fate and instead differentiate as PMCs (Zhao et al., 2002), resulting in an excess number of PMCs. In the second model, the signaling pathway is proposed to act earlier and in its absence there are excess PMCs resulting from additional cell divisions in the L2. Later, the excess PMC affect somatic cell differentiation (Canales et al., 2002). The coordination mechanism proposed in both models is that TPD1 is secreted by PMC to control the developmental fate of neighboring TA (model 1) or precursor somatic (model 2) cells by binding to the EMS1/EXS receptor (Feng and Dickinson, 2010a; Ma and Sundaresan, 2010). Two major issues remain unaddressed to test these models: (1) there is no experimental evidence to support TPD1 secretion; and (2) the protein localizations of TPD1 and EMS1/EXS are unknown early in anther development.

In rice, MSP1 (MULTIPLE SPOROCYTE1), an LRR-RLK, interacts with TDL1A (TPD1-like 1A) protein, its predicted ligand (Nonomura et al., 2003; Zhao et al., 2008). Rice *MSP1* and *TDL1A* genes are proposed to be homologs of *Arabidopsis EMS1/EXS* and *TPD1*, respectively. Interestingly, there are phenotypic differences between rice and *Arabidopsis* mutants. In rice *msp1* plants, both anther and ovule are affected (Nonomura et al., 2003), whereas no female phenotypes were reported in *Arabidopsis*. Although rice *msp1* anthers are phenotypically similar to *Arabidopsis ems1/ex*s and *tpd1* mutants, an RNA interference (RNAi) line directed against the rice *TDL1A* gene only has ovule defects (Zhao et al., 2008). These distinctions suggest that the proposed signaling pathway may have species-specific characteristics.

Maize *multiple archesporial cells 1* (*mac1*) mutants share the key phenotype of extra archesporial cells in both ovule and anther (Sheridan et al., 1996; Sheridan et al., 1999). *mac1* anthers contain just a single layer of somatic L2-d cells. Here, we report the cloning of *mac1*, which encodes a small secreted protein. Based on its sequence similarity and its mutant phenotype, maize *mac1* is the ortholog of rice *TDL1A*. In this study, we focused on the role of MAC1 during early anther development through characterizing the mutant phenotype, defining MAC1 protein localization and conducting double mutant analyses with other mutants that affect either anther development or meiosis. Our data indicate that MAC1 functions very early in anther development, prior to tapetal formation. MAC1 regulates the number of AR cells by preventing their overproliferation after specification. In addition, MAC1 is implicated in promoting periclinal cell division in the adjacent somatic cells, and may also act later, in the specification of tapetal cell fate.

MATERIALS AND METHODS

Plant material

The *mac1-1* mutant was provided by Bill Sheridan (University of North Dakota). The *mac1*, *afd1*, *am1* and *ocl4-1* mutants and inbred lines W23 and B73 were grown in Berkeley and Stanford, CA under field irrigation and fertilization or grown under greenhouse conditions. The *mac1-Y211* allele was recovered from a directed *Mutator* (*Mu*)-tagging experiment (supplementary material Fig. S1).

Molecular cloning

Genomic DNA was isolated from leaves (Dellaporta, 1994). Ten pairs of primers spanning the putative *mac1* gene were used to check the locus in the *mac1-1* mutant (supplementary material Table S1). The Southern blot experiment for characterization of *mac1-Y211* was performed as described previously (Nan and Walbot, 2009). The full length *mac1* cDNA was amplified using GeneRacer (Invitrogen, Carlsbad, CA, USA).

Phylogenetic analysis

mac1-related gene sequences were obtained from NCBI, and the virtual translation, full-protein sequences were aligned using ClustalW2 (http://www.ebi.ac.uk/Tools/msa/clustalw2/) with default options. The phylogenic tree was built using the maximum parsimony method with bootstrap values using PHYLIP (http://evolution.genetics.washington.edu/phylip.html).

RNA extraction and quantitative RT-PCR

Total maize RNA was isolated with TRIzol Reagent (Invitrogen), treated with DNase and then purified using an RNeasy kit (Qiagen, Valencia, CA, USA). For quantitative PCR, three biological samples for each tissue were assayed with three technical replicates, with the exception of pollen, silks and a 16-day embryo in which only a single biological sample was available. cDNA was synthesized using the Superscript III First Strand Synthesis System (Invitrogen) and quantitative PCR was conducted using the 2× Supermix qRT kit (Ambion, Austin, TX, USA) with primers F14 and R15 (supplementary material Table S1). Amplification of *cyanase* transcript was used as an internal control. PCR Miner (Zhao and Fernald, 2005) was used to calculate Ct values.

Protein extraction and western blot analysis

Total proteins were extracted using the TCA/acetone precipitation method and dissolved in Protein Extraction Reagent (Sigma, St Louis, MO, USA). A partial *mac1* cDNA, corresponding to amino acids 91-190 of the virtual translation, was used as an antigen to produce a rabbit polyclonal antibody using Genomic Antibody Technology (SDIX, Newark, DE, USA). The antibody was further affinity purified using a peptide column with amino acids 92-108 and used (1:100) in the western blot analysis.

Cytology

Spikelets were fixed in 3:1 (ethanol:acetic acid) and embedded with LR White resin (London Resin Company, UK). Semi-thin sections (1 μm) were stained with 1% Toludine Blue O in 1% Borax. For the *ocl4; mac1* double mutant, anthers were fixed in Bouin fixative, embedded and sectioned as described previously (Vernoud et al., 2009). The cytology of ovules was performed as described previously (Sheridan et al., 1996). Confocal microscopy and EdU incorporation were carried out as described previously (Kelliher and Walbot, 2011).

Immunohistochemistry

Spikelets were fixed in 4% formamide in 1× PBS and embedded in paraffin. Serial sections (10 μm) were placed on ProbeOn Plus slides (Fisher, Fairlawn, NJ, USA). The staining procedure was performed using affinity-purified MAC1 antibody (1:50) and anti-rabbit antibody (1:100) conjugated with alkaline phosphatase (Sigma).

Transient expression in onion epidermal cells

The full-length coding region and the predicted N-terminal signal peptide region were cloned into the vector pAVA120 (von Arnim et al., 1998). Plasmid DNA (5 μg) was bombarded into onion epidermal cells using a Biolistic PDS-1000/He device (Bio-Rad). To visualize GFP signal in the cell wall, samples were incubated with 20 mM PIPES-KOH (pH 7.0) for 8 hours before observation (Scott et al., 1999). Plasmolysis was induced by 0.8 M mannitol for 30 minutes.

RESULTS

Map-based cloning of the maize *mac1* gene

The original *mac1* mutant was isolated from an active *Mutator* stock and shown to be a monogenic recessive mutation on chromosome arm 10S. It was mapped between the breakpoint of the T9-10b translocation line and *oy1* (Sheridan et al., 1996). This interval is predicted between markers TIDP8865 and IDP8390, and comprises 900 kb (Fig. 2A). Among 14 predicted genes within this interval, the GRMZM2G027522 gene model shares similarity to the rice *TDL1A* and *Arabidopsis TPD1* genes with loss-of-function alleles causing phenotypes similar to the *mac1* mutant.

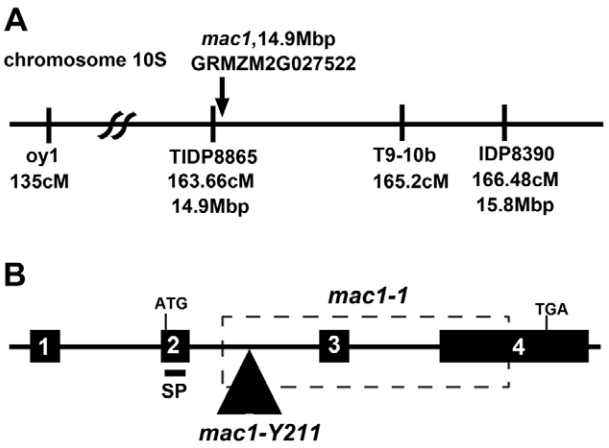

Fig. 2. Cloning and characterization of *mac1* alleles. (**A**) *mac1* was mapped to chromosome 10S, between genetic markers *oy1* and T9-10b (Sheridan et al., 1996). Inspection of the interval identified a candidate gene model, GRMZM2G027522, which shared similarity with rice *TDL1A*. (**B**) *mac1* gene structure. Exons are represented by black boxes. The deletion in *mac1-1* is outlined (broken rectangle), and the insertion of the *MuDR* element in the *mac1-Y211* allele is shown by a triangle (not drawn to scale). The first 32 amino acids are predicted to be a signal peptide (SP).

DNA sequence analysis uncovered a 1263 bp deletion in the *mac1* allele, starting within intron 2 and extending into exon 4 of GRMZM2G027522 (Fig. 2B). Attempts to sequence the transcript in the *mac1* mutant showed that intron 2 is not spliced, probably reflecting absence of the splice acceptor site. The resulting transcript has an in frame stop codon in the unspliced intron 2. The predicted encoded protein contains only the first 32 amino acids of the full-length functional protein, suggesting that *mac1* is a null mutation.

The *mac1-Y211* allele was isolated from a directed *Mutator* tagging screen (supplementary material Fig. S1). By DNA gel blot hybridization this allele contained a 4.9 kb autonomous *MuDR* insertion in intron 2 (Fig. 2B; supplementary material Fig. S1). Allelism analysis confirmed that *mac1-Y211* is allelic to the original allele, verifying that GRMZM2G027522 is the *mac1* gene (supplementary material Fig. S1). We now designate the original mutant allele as *mac1-1*.

Maize *mac1* is the ortholog of rice *TDL1A*

We cloned a 1405 bp full-length cDNA from the W23 inbred line (GenBank Accession Number JN247438). The *mac1* gene has four exons and the encoded protein is predicted to be 214 amino acids (22 kDa). MAC1 shares 58.7% and 39% similarity with rice TDL1A and *Arabidopsis* TPD1, respectively. Using SignalIP 3.0 software, the first 30 amino acids are a predicted cleavable signal peptide (Fig. 2B), which may target the protein into the endoplasmic reticulum for cellular export.

The MAC1 protein sequence was used in TBLASTN queries, and several related genes were found in maize, rice and *Arabidopsis* (cutoff E-value: e-10). Phylogenic analysis indicates that maize MAC1 and rice TDL1A form a branch in a clade that also contains *Arabidopsis* TPD1, whereas rice TDL1B occupies a more distant branch (supplementary material Fig. S2). Additionally, the region of the *TDL1A* gene on rice chromosome 12 is syntenic

to the maize chromosome 10 region where *mac1* resides. Considered together with the phylogeny, we conclude that *mac1* is the maize ortholog of the rice *TDL1A* gene.

mac1 affects cell proliferation in early anther development

Maize anther development is highly regular relative to anther length (Kelliher and Walbot, 2011), and this metric was used to compare fertile and sterile anthers. In transverse sections examined by light microscopy, anther lobes of very young anthers (~100 μm in length) contain a group of L2-derived cells (L2-d). At this stage, all L2-d cells appear similar in morphology, size and shape; subsequently, AR cells are found centrally as enlarged germinal cells. No significant difference was observed between fertile and *mac1* sterile anthers at this stage (Fig. 3A,F). At a slightly later stage (200-300 μm), fertile anthers contain one or two AR cells in each transverse section, surrounded by numerous L2-d somatic cells (Fig. 3B); subsequently, these L2-d cells divide periclinally (arrowhead in Fig. 3B), yielding the SPC and EN cells. Concurrently, the AR cells proliferate into several columns within the locule (Fig. 3C). Later in anther development (~700 μm in length), the secondary parietal cells divide periclinally (arrowhead in Fig. 3D) to form the TA that encircles the AR cells and the ML beneath the EN. During development, all cell layers divide anticlinally, increasing cell numbers in both the length and girth of each locule; for example, the number of EN cells increases from 8-10 (Fig. 3C) to 15-16 cells (Fig. 3E), as viewed in transverse sections. A few days prior to meiosis, each locule cell type has a distinct morphology (Fig. 3E): EP cells are elongated parallel to the long axis of the anther, EN cells are elongated 90° relative to the epidermal cells, the ML is flattened and the TA cells are cuboidal with a densely stained cytoplasm.

At the 300 μm stage the first clear *mac1* defect was observed in transverse section as an excess of AR cells enclosed by a single layer of subepidermal L2-d cells (Fig. 3G,K). Periclinal division of L2-d subepidermal cells in *mac1* is delayed (Fig. 3H-L). The mutant L2-d cells do divide anticlinally; in transverse section, the subepidermal cell number is about 15-16 in *mac1* anthers (Fig. 3I,L), so only the periclinal division is suppressed. Later, just prior to meiosis, some *mac1* L2-d sub-epidermal cells divide irregularly (supplementary material Fig. S4), to form several cell layers with unclear cell identity. At later stages in *mac1*, the subepidermal layer shares some characteristics with EN; however, cells with characteristics of the ML or TA layers are never observed (Fig.

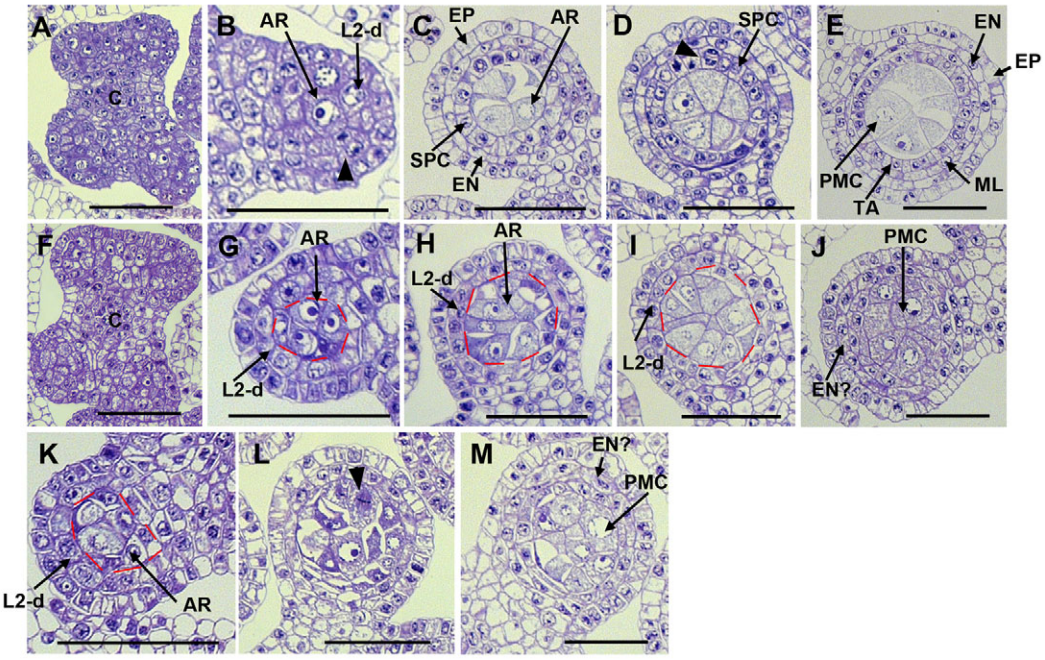

Fig. 3. Phenotypic characterization of male anther development in *mac1* mutants and fertile siblings. Transverse sections of anther lobes from wild-type (A-E), *mac1-1* mutant (F-J) and *mac1-Y211* mutant (K-M) at successive developmental stages. (**A**,**F**) 100 μm anthers. There is no significant difference between wild-type (A) and mutant (F) at this stage. (**B**,**G**,**K**) 200-300 μm anthers: in a wild-type anther (B), the archesporial cells (ARs) were already differentiated and only one or two AR are visible in transverse sections, surrounded by one layer derived from L2-derived (L2-d) cells. One L2-d cell is dividing periclinally (arrowhead) to form secondary parietal cells (SPCs) and endothecium (EN). In the *mac1* mutants, excess AR cells (red circle) are apparent in both *mac1-1* (G) and *mac1-Y211* (K) anthers. (**C**,**H**,**L**) 500 μm anthers: in a wild-type anther (C), long and thin EN cells were differentiated and SPCs enclose four or five AR cells. In both *mac1* mutant alleles (H,L), increased cell division in the AR cells (supplementary material Fig. S3) has generated excess ARs. The L2-d cells remain a single layer encircling AR cells (red outline). Arrowhead in L indicates a dividing AR cell. (**D**,**I**) 700 μm anthers: SPCs are dividing periclinally (arrowhead in D) in a wild-type anther to form the middle layer (ML) and the tapetum (TA). By contrast, in the *mac1-1* (I) at this stage, the L2-d layer exhibits no periclinal divisions. Note that all AR cells are distinctively distinguishable from the two-layer anther wall in G-I. Red outline in I indicates the domain of AR cells. (**E**,**J**,**M**) 1 mm anthers: in wild type, the central pollen mother cells (PMCs) are surrounded by four somatic anther wall layers: TA, ML, EN and epidermis (EP). In both *mac1-1* (J) and *mac1-Y211* (M), the single subepidermal layer began dividing in a disorderly fashion prior to meiosis. A layer of long thin cells resembling EN forms; however, differentiation of ML and TA was never observed in either mutant. Instead, a few cells of unknown identity form a two layer wall in *mac1* mutants (also see supplementary material Figs S4, S5). The distinctive border observed between PMC cells and the anther wall disintegrates at this stage in *mac1* mutants. Scale bars: 50 μm.

3J,M; supplementary material Fig. S5). Because the two alleles showed similar phenotypes, the following analyses were carried out using the *mac1-1* allele, unless otherwise specified.

Confocal microscopy was used to compare reconstructions of sterile and fertile sibling anthers. A longitudinal optical section of fertile anthers (425 μm stage) showed clearly that AR cells are enclosed by three somatic cell layers: EP, EN and SPC (Fig. 4A). By contrast, a 425 μm *mac1-1* anther had an excess number of AR cells enclosed by only the EP and L2-d cells (Fig. 4B). To examine the cell proliferation rate during anther development, EdU was incorporated into replicating DNA during S phase to label actively dividing cells (Fig. 4C,D). In *mac1*, the AR cells proliferate at least twofold more frequently (Fig. 4E). Consequently, *mac1* anthers have accumulated three times more AR cells in a locule compared with fertile anthers at the 600 μm stage (supplementary material Fig. S3).

mac1 does not affect meiotic cell identity

It has been inferred that meiosis arrests in prophase I in *mac1-1* (Golubovskaya et al., 1992a; Sheridan et al., 1999). Here, we examined RAD51 loading onto chromosomes. RAD51 is a RecA-like protein involved in homologous recombination, and it exists in foci on chromosomes during prophase I (Franklin et al., 1999). RAD51 loading is normal in the *mac1-1* mutant (supplementary material Fig. S6). Furthermore, meiotic progression in *mac1-Y211* is typically arrested before metaphase I; however, a few mutant meiocytes reach metaphase II (supplementary material Fig. S7). All anthers from both mutant alleles are completely sterile. We conclude that *mac1* mutant meiocytes have the correct cell identity in both mutants but meiosis fails; because many mutants with tapetal defects exhibit 'failure to thrive' syndromes, we speculate that the absence of a functional tapetal layer results indirectly in meiotic arrest.

We further constructed double mutants with two meiotic genes, *am1* (*ameiotic1*) and *afd1* (*absence of first division1*). In *am1-1* anthers and ovules, meiocytes conduct mitosis instead of meiosis (Golubovskaya et al., 1992b; Golubovskaya et al., 2006). In the *afd1* mutant, the first division is absent and sister chromatids separate at metaphase I. The offspring of self-pollinated *mac1*/+; *am1*/+ and *mac1*/+; *afd1*/+ double heterozygous stocks were examined (supplementary material Tables S2, S3). In each family, the segregation of fertile and sterile plants was 9:7, as expected, and megaspore mother cells (MMC) isolated from single ovules on sterile plants were examined by light microscopy. In both *mac1/mac1; am1/am1* and *mac1/mac1; afd1/afd1* double mutant plants, multiple MMCs were observed, which is characteristic of *mac1*. For the *mac1/mac1; afd1/afd1* double mutant, 1001 MMCs at various stages were observed in 183 ovules (supplementary material Table S4), showing an average of 5.5 MMCs in double mutants compared with one such cell per ovule in wild-type plants and nine MMCs in *mac1* plants (Sheridan et al., 1996). By comparison, in anthers there was approximately a two- to threefold increase of PMCs in *mac1* compared with fertile plants. In addition, as meiosis started, *am1* or *afd1* meiotic phenotypes appeared in both double mutants (supplementary material Figs S8, S9), suggesting that *mac1* acts independently of both meiosis genes. As shown in supplementary material Tables S2 and S3, the segregation ratios were 9:3:3:1. The additive nature of phenotypes in both double mutants confirms that PMCs in *mac1* mutants can enter the meiotic cell cycle appropriately.

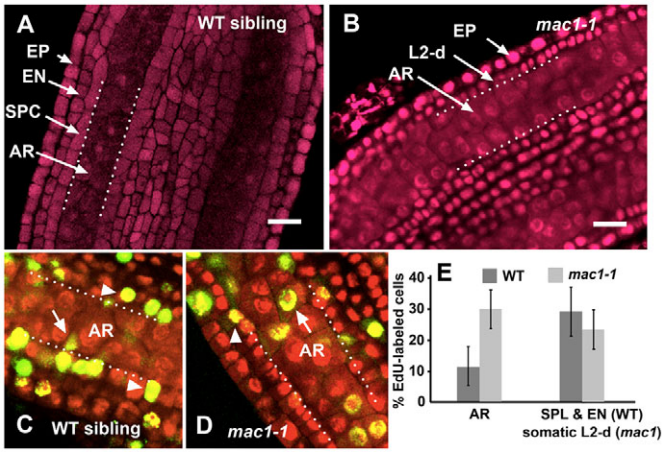

Fig. 4. Confocal images in a longitudinal optical section of wild-type and *mac1* mutant anthers. (**A**) In the wild-type anther (425 μm), four cell layers are present – the epidermis (EP), endothecium (EN), secondary parietal cells (SPC) and archesporial cells (AR). Two or three columns of AR cells are present in the center of the locule. (**B**) *mac1-1* mutant anthers (425 μm) have only two somatic cell layers: EP and a single somatic cell layer, which encircle extra columns of AR cells. There are up to five columns of AR cells. These extra AR cells are similar in size and morphology. Scale bars: 30 μm in A,B. (**C**,**D**) Confocal images of EdU-labeled anthers to mark actively dividing cells. (C) In wild-type anther (300 μm), few AR cells are EdU labeled in a 5 hour treatment (arrow), but many secondary parietal cells are (arrowheads). (D) In *mac1* anthers (310 μm), more AR cells are EdU-labeled (arrow), whereas few somatic cells are labeled (arrowhead). (**E**) Average percentage of AR and L2-d somatic cells that are EdU labeled in wild-type and *mac1* anthers (*n*=15). Data are mean±s.e.m.

mac1 transcript is highly expressed in anthers and root tissue

mac1 mRNA levels in the anther, ear and other organs were examined by quantitative RT-PCR (Fig. 5A). The *mac1* transcript level is low in anthers smaller than 500 μm and peaks during meiosis, then drops off sharply after meiosis is completed. *mac1* transcripts are low in the ear but exhibit high expression in the root; no expression was detected in pollen, silk, embryos (16 days post fertilization), juvenile leaf or stem (10 days post germination). This pattern is similar to rice *TDL1A* expression, except that the rice transcript is also present in embryos (Zhao et al., 2008). By contrast, the RNA expression of the rice *TDL1B* gene is not consistent with its putative homolog in maize; there is no RNA expression in maize root, anther and ear tissues when assessed using quantitative RT-PCR.

To check whether *mac1* roots have a scorable defect, we examined primary root growth and performed confocal imaging of maize roots; we found no obvious difference between wild-type sib and *mac1* mutant plants (data not shown).

In anthers, MAC1 protein is primarily localized to archesporial cells

MAC1 contains a predicted cleavable signal peptide; the processed protein has a predicted mass of 18.6 kDa. We raised a polyclonal antibody against a partial sequence of MAC1 (amino acids 91-190). The 91-190 amino acid antigen affinity-purified antibody showed poor specificity (supplementary material Fig. S10). To improve it, we purified the antiserum with an affinity column coupled with a MAC1 peptide (amino acids 92-108). This affinity-purified antibody specifically recognizes an anther protein of ~18

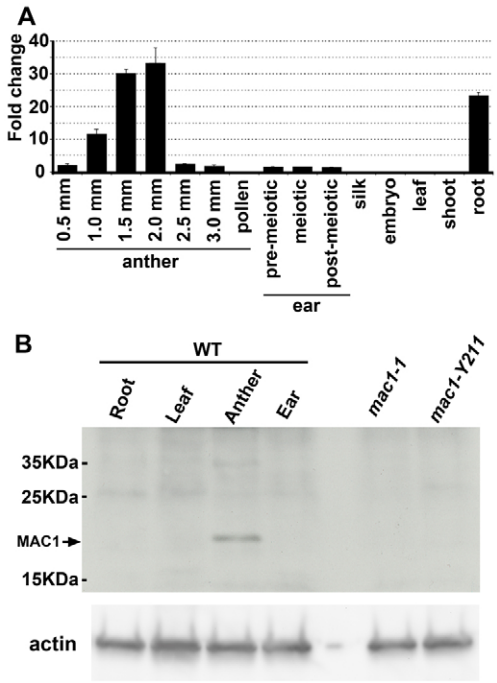

Fig. 5. Quantification of *mac1* mRNA transcript level by qRT-PCR and western blot analysis of MAC1 protein. (**A**) *mac1* mRNA transcript levels in anthers, ears and other maize organs. The *y*-axis is *mac1* RNA expression relative to the post-meiotic ear. Very little *mac1* transcript is present at 500 μm. *mac1* expression increases after locular cell types have been established (1.0 mm anthers) and peaks after meiocytes enter meiosis (1.5-2.0 mm anthers). Transcript level drops off sharply after meiosis (2.5 mm). Data are mean±s.e.m. (**B**) Western blot probed with affinity-purified anti-MAC1 antibody showing that MAC1 is present in wild-type anthers but absent in *mac1* mutant anthers. Actin levels were used as loading controls.

kDa; this band is absent in anther protein extracts from both mutants (Fig. 5B). We conclude that the mature MAC1 protein is about 18 kDa and that both mutant alleles are null mutations. Although *mac1* is required for normal embryo sac development in ears, the 18 kDa protein was not detected in the ear protein sample. Unlike the anther, which is rich in sporogenous tissue, immature ears are nearly all somatic cells; we propose that the level of protein in ears is too diluted to be detected.

Immunolocalization assays using the peptide-affinity purified antibody were performed to elucidate MAC1 protein distribution. In 150 μm anthers, MAC1 protein was first visible in a few L2-d cells with weaker signals diffusely present in the four anther lobes, surprisingly including the EP and the connective tissue between the abaxial- and adaxial locules (Fig. 6A). Slightly later in development (300-400 μm), the MAC1 signal becomes more concentrated in the central cells of each locule, corresponding to the location of AR cells (Fig. 6B). In some sections, a weaker MAC1 signal was also observed in some epidermal cells at the outer ridge of anther locules (Fig. 6C). After all cell types have been established by 750 μm, the MAC1 signal was even stronger in the AR cells with a much weaker signal in the adjacent cells; it is possible that the low signals outside the AR cells here and at earlier stages represent diffusion of MAC1 protein after secretion by AR cells (Fig. 6D,E). No MAC1 signal was detected in the *mac1-1* mutant (Fig. 6F), validating that the signals in fertile anthers represent detection of MAC1 protein.

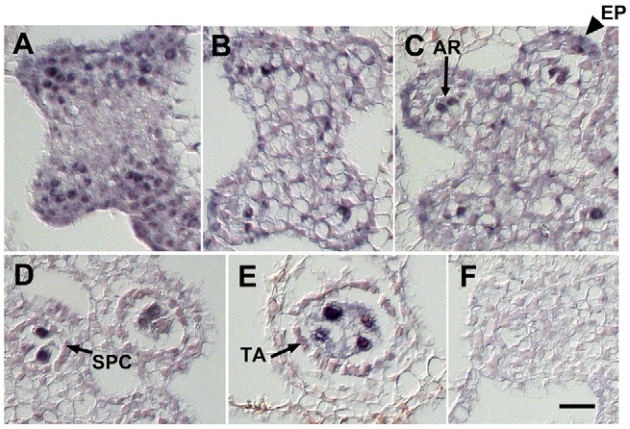

Fig. 6. Immunohistochemical analysis of MAC1 protein at different stages of anther development. (A-E) Transverse sections of wild-type anthers. (**A**) MAC1 protein (purple signal) is detected primarily in L2 cells in 150 μm anthers. (**B**,**C**) Later (300 μm anther), the MAC1 signal is strengthened in AR cells (arrow); epidermal cells at the outer edges of anther locules had weaker signals (arrowhead). (**D**,**E**) MAC1 protein becomes more restricted to the AR cells and weaker signals are observed in the secondary parietal cell (SPC) (arrow in D) and the tapetal layer (TA) (arrow in E). (**F**) Control experiment using a *mac1-1* mutant anther (400 μm) in which there is only faint background signal. Scale bar: 20 μm.

MAC1 protein is secreted from onion cells

Although MAC1 and its homologs are predicted to be secreted proteins, this feature has not been established experimentally. To determine the subcellular localization of MAC1, GFP was fused either to the C terminus of MAC1 or to the putative signal peptide (SP) (Fig. 7A) and expressed in onion epidermal cells. The control GFP vector exhibited both cytoplasmic and nuclear fluorescence (Fig. 7B), consistent with a previous report (Chiu et al., 1996). The SP-GFP fusion protein was secreted into the extracellular space between cells (Fig. 7C,D). We propose that the fusion protein is processed and secreted via the vesicular secretory pathway as SP-GFP signals were also observed in the endoplasmic reticulum around the nucleus (Fig. 7C). When the full-length MAC1 was fused to the GFP, the signal was observed only in the endoplasmic reticulum (Fig. 7E); no extracellular signal was apparent. It is likely that the large fusion protein (45 kDa) is unable to move through the cell wall (Baron-Epel et al., 1988). To discern whether the MAC1-GFP signal is secreted but hampered in movement by exclusion from the cell wall, onion epidermis was treated with hypertonic solution. After plasmolysis, it is evident that some MAC1-GFP fusion protein is associated with the cell wall (arrowhead in Fig. 7I), as well as the Hechtian strands (arrow in Fig. 7I). This was not observed with the GFP control (Fig. 7G,H). These observations indicate that MAC1 protein can be secreted via the endoplasmic reticulum-mediated secretory system.

Can extra somatic cell divisions compensate for the somatic defects of *mac1*?

Maize *ocl4* (*outer cell layer 4*) encodes a transcription factor of the HD-ZIP class IV family, which is specifically expressed in the EP of numerous organs. In the *ocl4* mutant, anthers begin their development normally but an additional periclinal cell division occurs after the L2-d cells divide periclinally to form the EN and SPC. The presumptive EN divides periclinally again in the locular

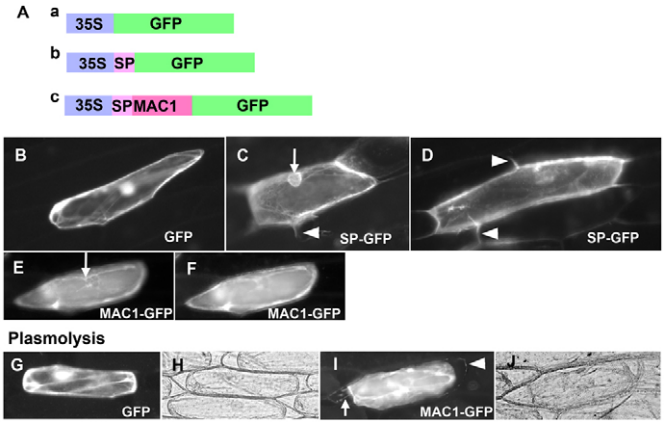

Fig. 7. Subcellular localization of MAC1 protein by transient expression in onion epidermis. (**A**) Constructs used in this study. (**B**) An onion epidermal cell transiently expressing the GFP control. The GFP signal was distributed in cytoplasm and nucleus. (**C**,**D**) Transient expression of the SP-GFP construct. The chimeric protein is secreted to the extracellular space (arrowheads) via the secretory pathway. Arrow indicates the nucleus surrounded by endoplasmic reticulum. (**E**,**F**) Different focal planes of the same cell expressing the MAC1-GFP construct. The signal was distributed in the endoplasmic reticulum around the nucleus (arrow). (**G**,**H**) Bright-field (H) and corresponding fluorescence image (G) of a plasmolyzed cell expressing the GFP control. (**I**,**J**) Bright-field (J) and corresponding fluorescence image (I) of a plasmolyzed cell expressing the MAC1-GFP construct. The GFP signal is present in the endoplasmic reticulum, Hechtian threads (arrow) and extracellular space (arrowhead).

bulge, leading to the formation of two cell layers with EN characteristics such as accumulation of starch granules (Vernoud et al., 2009) (Fig. 8B). At the same stage, in the *mac1* mutant, one L2 layer is present subepidermally, but only late in premeiotic anther development does it exhibit any EN-like characteristics (Fig. 8C). In the *mac1-1; ocl4* double mutant, excess AR cells are observed with disordered somatic cells around them as observed in *mac1*. Two EN-like layers with starch granules also develop (Fig. 8D). Taken together, these result indicate that the two mutant phenotypes are additive and that extra subepidermal cells generated by the *ocl4* defect do not lead to differentiation of ML or TA types in the absence of MAC1.

To ascertain the timing of phenotypic deviations more precisely, *mac1; ocl4* double mutant anthers were observed by confocal microscopy. In the *ocl4*, the extra periclinal division occurs after the initial L2-d periclinal division (Vernoud et al., 2009), a stage corresponding to ~400-500 μm anthers (Kelliher and Walbot, 2011). In fertile anthers at this stage, the EN and SPC have already developed (Fig. 8E), whereas, in *mac1*, only a single layer of L2-d subepidermal cells exists (Fig. 8F). In the double mutant, however, some cells in the L2-d subepidermal layer divide in 500 μm anthers (Fig. 8G, arrowhead). These divisions in the double mutant take place at about the same time as formation of the extra EN layer in the single *ocl4* mutant; the number of AR cells resembles the *mac1* mutant (Fig. 8G). Later, a burst of irregular cell division occurs in the double mutant to form unorganized cell layers with unclear cell identity, similar to *mac1* (Fig. 8H). In summary, the double mutant shows an additive phenotype, indicating these two genes are probably acting independently to influence somatic cell division patterns in anther locules.

DISCUSSION

Analysis of *mac1* supports the theory that cell position, not lineage, is crucial for cell fate determination in anther locules

Plant organ development requires communication between cell layers to coordinate tissue differentiation (Fletcher, 2002; Feng and Dickinson, 2010b; Ma and Sundaresan, 2010). We demonstrate that early in anther ontogeny, MAC1 suppresses AR cell proliferation and that it is also required to promote periclinal division in the adjacent L2-d cells. The early roles of MAC1 suggest a function in regulating cell division rather than in guiding the SPC and TA differentiation to suppress trans-differentiation into PMC. In support of our conclusion, by immunolocalization, MAC1 is located primarily in the initial AR cells, with a diffuse gradient across the microsporangium. We demonstrate that MAC1 is a secreted protein and hypothesize that AR cells are a ‘signaling center’ from their inception. We further hypothesize that the dual early roles result from the secreted MAC1 protein via binding to a receptor kinase(s) in the AR cells to regulate their proliferation frequency and binding to a different receptor kinase(s) in the adjacent L2-d cells to regulate their periclinal division. These L2-d cells continue anticlinal cell divisions in *mac1* mutants; therefore, the role of MAC1 is specific to promoting their periclinal division rather than being a general regulator of L2-d cell proliferation. Early steps in anther ontogeny have not yet been investigated in *tpd1 Arabidopsis* or *tdl1a* rice, whereas roles of MAC1 at later stages cannot be assessed in these *mac1* mutants because cell differentiation is disrupted so early. Therefore, we cannot exclude the possibility that *mac1* may induce the division of secondary parietal cells and then determine the fate of tapetal cells.

The *ocl4* gene plays a role in suppressing additional periclinal division in EN precursors. In the absence of OCL4, these cells divide periclinally once to form an extra EN-like cell layer. These divisions occur in the outer locule arc distant from the central vascular column in the center of each anther (Vernoud et al., 2009). OCL4 is a transcription factor expressed exclusively in epidermal cells, suggesting that the signal(s) inhibiting periclinal division in EN cells is generated in the overlying layer. Double mutant analyses of *mac1* and *ocl4* demonstrated additive phenotypes, suggesting that these genes act independently in different pathways. The L2-d layer encircling excess AR cells in the *mac1* mutant does not divide periclinally, a feature that we reasoned reflects the absence of MAC1. The absence of periclinal divisions may be reinforced by the normal OCL4-dependent signaling pathway generated by the overlying EP. In *mac1; ocl4* double mutants, the L2-d cells do perform periclinal divisions starting at about the same stage as the extra periclinal divisions characteristic of *ocl4*. These observations suggest that the subepidermal L2-d cells in *mac1* can respond to the signal from EP that inhibits additional division. Collectively, our analyses suggest that both EP and AR cells regulate the timing and location of periclinal divisions in L2-d cells (Fig. 9). The AR secretes a promoting factor required for the single periclinal divisions of L2-d subepidermal cells, and then the EP makes a suppressor acting on the outer layer after this division. Our observations provide strong evidence that cell-cell signaling is important in anther ontogeny and that signaling processes based on cell position rather than lineage are the major factor regulating differentiation of the L2-d cells into EN and SPC. Similar processes, perhaps involving some of the same proteins, may regulate the later step of secondary parietal periclinal division to generate the ML and TA.

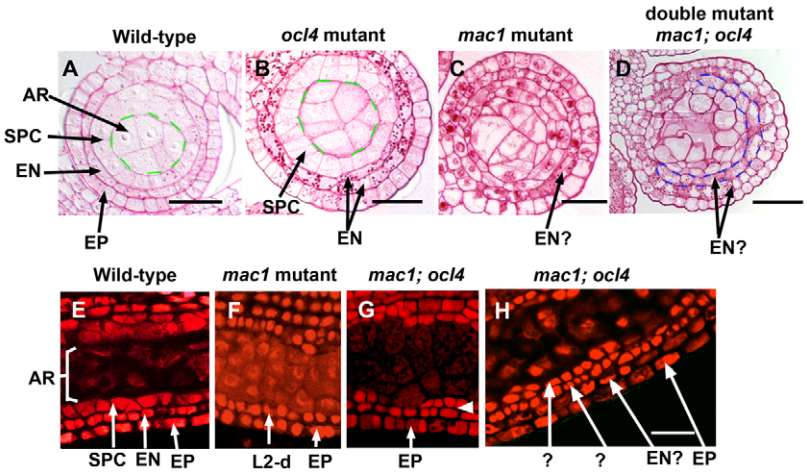

Fig. 8. Phenotypic characterization of the *mac1; ocl4* double mutant. (A-D) Transverse section of anther lobes. (**A**) In the wild-type anther (500 μm), four cell types are present: the epidermis (EP), endothecium (EN), secondary parietal cells (SPC) and archesporial cells (AR). The EN cells are elongated and have started to accumulate starch granules. (**B**) In the *ocl4* mutant, after L2-d cells have divided periclinally to form two layers, the outer layer divided periclinally again to form two EN-like cell layers. (**C**) In the *mac1* mutant, excess AR cells are observed. An EN-like layer with starch granules forms from a few cell layers with unknown identity. (**D**) In the *mac1; ocl4* double mutant, excess AR cells are present with unorganized somatic cells surrounding them. In addition, two EN-like layers form (blue dotted lines). The border of AR cells is evident in both wild-type (A) and the *ocl4* mutant (B) (green dotted lines); however, it becomes disordered in the *mac1* mutant (C) and *mac1; ocl4* double mutant (D). (E-H) Confocal images of longitudinal optical sections of anthers. (**E**) A wild-type locule (500 μm anther) illustrates that EN and SPC have differentiated. (**F**) A 450 μm *mac1* anther shows that excess AR cells enclosed by one layer of cells derived from L2 (L2-d) and EP. (**G**) A *mac1; ocl4* double mutant anther (500 μm) shows an increased number of AR plus irregular patches of two somatic cell layers (arrowhead). (**H**) A *mac1; ocl4* double mutant anther (1 mm) exhibits a burst of cell divisions as seen in *mac1* mutant. Scale bars: 20 μm.

Maize *mac1* encodes a small protein similar to rice TDL1A and *Arabidopsis* TPD1

We report here that *mac1* encodes a small protein with an N-terminal signal peptide and that it shares similarity with rice *TDL1A* and *Arabidopsis TPD1* genes. Both *mac1* and rice *tdla-RNAi* mutants share the ovule development defect of excess MMCs (Sheridan et al., 1996; Zhao et al., 2008). *tdla-RNAi* rice exhibits normal anther development, a result interpreted to be consequence of failure to express sufficient RNAi in anthers (Zhao et al., 2008). Based on phenotypic similarity, syntenic chromosomal locations and phylogenic analysis, we conclude that maize *mac1* is the ortholog of the rice *TDL1A* gene.

Both TDL1A and TPD1 were predicted to be secreted ligands, and they interact with the LRR-RLKs MSP1 and EMS1/EXS in rice and *Arabidopsis*, respectively (Canales et al., 2002; Zhao et al., 2002; Yang et al., 2003; Jia et al., 2008; Zhao et al., 2008). The rice *msp1* mutant displayed an excessive number of both male and female sporogenous cells; anther wall layers were disordered and the TA layer was absent completely (Nonomura et al., 2003). These phenotypes are similar to maize *mac1* in both anthers and ovules. By contrast, the *Arabidopsis tpd1* or *ems1/exs* mutants show defects only in anthers (Zhao et al., 2002; Yang et al., 2003; Feng and Dickinson, 2010a). Therefore, there are differences in the signaling pathways for male and female reproductive organ development in grasses and dicots.

MAC1 is required early in anther locule development

In *ems1* and *tpd1 Arabidopsis* mutants, excess sporogenous cells appeared at stage 5 anthers and the TA layer was missing (Zhao et al., 2002; Yang et al., 2003). The number of AR in these mutants is similar to the sum of the TA and the AR in fertile anthers (Zhao et al., 2002). These data were invoked to propose that the TPD1-EMS1 signaling pathway specifies TA cell fate after the periclinal division of the SPC: in effect, suppressing the germinal fate in the tapetal cells (Feng and Dickinson, 2010a; Ma and Sundaresan, 2010). Exploiting the large size of maize anthers during the initial steps of cell fate setting, we find that *mac1* anthers contain excess AR from the earliest stages examined (<300 μm) and that these AR cells subsequently proliferate at more than twice the rate observed in fertile anthers throughout the period before SPCs in fertile anthers would divide to generate the tapetal layer. Therefore, at least in maize, MAC1 functions as a suppressor of AR proliferation in an autoregulatory circuit. Absence of this suppressive function is sufficient to explain the excess PMC phenotype without invoking trans-differentiation of a newly formed tapetal layer.

By confocal analysis, maize ARs are specified before 300 μm within dozens of L2-derived somatic cells in each lobe. There was no evidence for a single hypodermal cell dividing asymmetrically to form a founding primary parietal cell and a single primary sporogenous cell (Kelliher and Walbot, 2011). How AR cell fate is set in maize remains largely unknown. In *Arabidopsis* the transcription factor *SPOROCYTELESS/NOZZLE* (*SPL/NZZ*) promotes AR specification (Yang et al., 1999; Ito et al., 2004). *SPL/NZZ* is thought to interact with two LRR-RLKs, *BARELY ANY MERISTEM 1* and *2* (*BAM1* and *BAM2*) (Hord et al., 2006). Interestingly, both maize and rice lack a homolog of SPL/NZZ, which provides a second example in which grasses, and perhaps monocots in general, regulate the male component of reproduction differently from *Arabidopsis*.

There are some parallels between the role of MAC1 in suppressing AR proliferation and the role of *CLAVATA3* (*CLV3*) in shoot apical and floral meristems (Willmann, 2000; Rojo et al., 2002). CLV3 acts as a negative regulator to control the number of

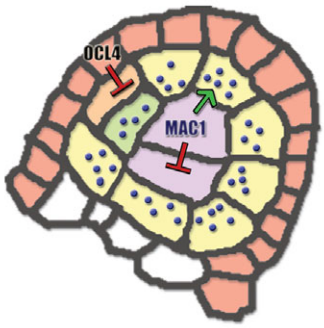

Fig. 9. Model of MAC1 function in the developing anther. *mac1* is expressed in the archesporial (AR) cells and acts to inhibit the uncontrolled proliferation of AR and to promote the periclinal division of L2-d cells. Later in development, MAC1 is implicated in differentiation or stabilization of the TA. *ocl4*, which is expressed in the epidermis, acts to repress extra periclinal divisions in the L2-d cells, particularly in the endothecium. The action of *ocl4* to repress and *mac1* to promote periclinal divisions in L2-d cells must be tightly coordinated spatially and temporally to result in the correct anther anatomy.

stem cells (Brand et al., 2000). CLV3 is a secreted protein that functions as a ligand for the CLV1-CLV2 receptor kinase complex (Willmann, 2000; Sharma et al., 2003). CLV3 activates a signal transduction cascade to restrict expression of the WUSCHEL (WUS) transcription factor, a protein that promotes stem cell formation and also provides a negative-feedback regulation on CLV3 expression (Muller et al., 2006). The size of the apical meristem cell population is controlled by the balance of CLV3 and WUS expression. If this analogy holds in anther locules, then a second factor opposing MAC1 action is predicted to promote AR proliferation.

mac1 promotes formation of the somatic anther wall

When excess AR cells are first observed in *mac1*, there is only one layer of encircling L2-d cells, a state that persists until close to the start of meiosis (Sheridan et al., 1999; Abramova et al., 2002). MAC1 suppresses AR proliferation, but it is also required to promote periclinal division in the L2-d cells. In *mac1* mutant, L2-d cells divide regularly anticlinally to sustain anther growth. At the stage when all five cell types are present in normal locules, the *mac1* L2-d cells begin to divide irregularly (not strictly in the periclinal plane) to form patches of multilayered somatic wall tissue. We attribute the absence of early periclinal L2-d cell divisions in *mac1* anthers to the absence of MAC1 protein secretion by the central AR cells. The divisions near the onset of meiosis could arise from a different signal or mechanism.

When TPD1 is expressed ectopically in wild-type *Arabidopsis*, the number of carpel cells increased significantly, which supports the positive role that this type of protein can have on somatic cell proliferation (Yang et al., 2005). TPD1 activation of cell division in the transgenic carpel is dependent on its receptor, EMS1/EXS (Yang et al., 2005). Feng and Dickinson (Feng and Dickinson, 2010a) expressed EMS1 under the control of the A9 tapetal promoter in *ems1* plants and found that locular peripheral cells (similar to our designation of L2-d cells) could respond late in anther ontogeny to differentiate as functional tapetal cells. If TPD1 is the ligand late in development, this supports a third role for the triad of MAC1/TDL1A/TPD1 proteins in regulating tapetal differentiation. We hypothesize one or more kinases may interact with MAC1 in maize to support its multiple roles in anther and ovule.

Acknowledgements
We thank Bill Sheridan (University of North Dakota) and David Duncan for *mac1* mutants; David Duncan was supported by a VPUE summer research award from Stanford University to conduct the directed tagging and initial analysis of new mutants of *mac1*. We thank Ling Meng and Peggy G. Lemaux (UC Berkeley) for help with onion transient expression assay, and Jennifer Fletcher (Plant Gene Expression Center, USDA) for her gift of pAVA120. We thank Wann-Neng Jane and Plant Cell Biology Core Lab (IPMB, Academia Sinica) for help in anther sectioning. We thank Jihyun Moon (UC Berkeley) for her comments on the manuscript.

Funding
This work was supported by a grant from the US National Science Foundation [07-01880].

Competing interests statement
The authors declare no competing financial interests.

Supplementary material
Supplementary material available online at
http://dev.biologists.org/lookup/suppl/doi:10.1242/dev.077891/-/DC1

References

Abramova, L. I., Avalkina, N. A., Golubeva, E. A., Pyzhenkova, Z. S. and Golubovskaya, I. N. (2002). Embryological effect of the mac1 mutation in *Zea Mays* (Poacaae). *Bot. J. (Russ.)* **87**, 28-32.
Albrecht, C., Russinova, E., Hecht, V., Baaijens, E. and de Vries, S. (2005). The *Arabidopsis thaliana* SOMATIC EMBRYOGENESIS RECEPTOR-LIKE KINASES1 and 2 control male sporogenesis. *Plant Cell* **17**, 3337-3349.
Baron-Epel, O., Gharyal, P. K. and Schindler, M. (1988). Pectins as mediators of wall porosity in soybean cells. *Planta* **175**, 389-395.
Bedinger, P. A. and Fowler, J. E. (2009). The maize male gametophyte. In *Handbook of Maize: Its Biology* (ed. J. L. Bennetzen and S. C. Hake), pp. 57-77. New York, USA: Springer.
Bhatt, A. M., Canales, C. and Dickinson, H. G. (2001). Plant meiosis: the means to 1N. *Trends Plant Sci.* **6**, 114-121.
Brand, U., Fletcher, J. C., Hobe, M., Meyerowitz, E. M. and Simon, R. (2000). Dependence of stem cell fate in Arabidopsis on a feedback loop regulated by CLV3 activity. *Science* **289**, 617-619.
Canales, C., Bhatt, A. M., Scott, R. and Dickinson, H. (2002). EXS, a putative LRR receptor kinase, regulates male germline cell number and tapetal identity and promotes seed development in Arabidopsis. *Curr. Biol.* **12**, 1718-1727.
Chiu, W.-l., Niwa, Y., Zeng, W., Hirano, T., Kobayashi, H. and Sheen, J. (1996). Engineered GFP as a vital reporter in plants. *Curr. Biol.* **6**, 325-330.
Colcombet, J., Boisson-Dernier, A., Ros-Palau, R., Vera, C. E. and Schroeder, J. I. (2005). Arabidopsis SOMATIC EMBRYOGENESIS RECEPTOR KINASES1 and 2 are essential for tapetum development and microspore maturation. *Plant Cell* **17**, 3350-3361.
Dellaporta, S. (1994). Plant DNA miniprep and microprep. In *The Maize Handbook* (ed. M. Freeling and V. Walbot), pp. 522-525. New York, USA: Springer.
Feng, X. and Dickinson, H. G. (2010a). Tapetal cell fate, lineage and proliferation in the Arabidopsis anther. *Development* **137**, 2409-2416.
Feng, X. and Dickinson, H. G. (2010b). Cell-cell communication in plant reproduction. *Biochem. Soc. Trans.* **38**, 571-576.
Fletcher, J. C. (2002). Shoot and floral meristem maintenance in arabidopsis. *Annu. Rev. Plant Biol.* **53**, 45-66.
Franklin, A. E., McElver, J., Sunjevaric, I., Rothstein, R., Bowen, B. and Cande, W. Z. (1999). Three-dimensional microscopy of the Rad51 recombination protein during meiotic prophase. *Plant Cell* **11**, 809-824.
Golubovskaya, I., Avalkina, N. A. and Sheridan, W. F. (1992a). Effects of several meiotic mutations on female meiosis in maize. *Dev. Genet.* **13**, 411-424.
Golubovskaya, I. N., Grebennikova, Z. K. and Avalkina, N. A. (1992b). New allele of ameiotic1 gene in maize and problem of gene control of meiosis initiation in high plants. *Genetika (Russ.)* **27**, 137-146.
Golubovskaya, I. N., Hamant, O., Timofejeva, L., Wang, C. J., Braun, D., Meeley, R. and Cande, W. Z. (2006). Alleles of afd1 dissect REC8 functions during meiotic prophase I. *J. Cell Sci.* **119**, 3306-3315.
Hord, C. L., Chen, C., Deyoung, B. J., Clark, S. E. and Ma, H. (2006). The BAM1/BAM2 receptor-like kinases are important regulators of Arabidopsis early anther development. *Plant Cell* **18**, 1667-1680.
Ito, T., Wellmer, F., Yu, H., Das, P., Ito, N., Alves-Ferreira, M., Riechmann, J. L. and Meyerowitz, E. M. (2004). The homeotic protein AGAMOUS controls microsporogenesis by regulation of SPOROCYTELESS. *Nature* **430**, 356-360.

Jia, G., Liu, X., Owen, H. A. and Zhao, D. (2008). Signaling of cell fate determination by the TPD1 small protein and EMS1 receptor kinase. *Proc. Natl. Acad. Sci. USA* **105**, 2220-2225.
Kelliher, T. and Walbot, V. (2011). Emergence and patterning of the five cell types of the *Zea mays* anther locule. *Dev. Biol.* **350**, 32-49.
Kiesselbach, T. A. (1949). *The Structure and Reproduction of Corn*. Cold Spring Harbor, NY: Cold Spring Harbor Laboratory Press.
Ma, H. (2005). Molecular genetic analyses of microsporogenesis and microgametogenesis in flowering plants. *Annu. Rev. Plant Biol.* **56**, 393-434.
Ma, H. and Sundaresan, V. (2010). Development of flowering plant gametophytes. *Curr. Top. Dev. Biol.* **91**, 379-412.
Muller, R., Borghi, L., Kwiatkowska, D., Laufs, P. and Simon, R. (2006). Dynamic and compensatory responses of Arabidopsis shoot and floral meristems to CLV3 signaling. *Plant Cell* **18**, 1188-1198.
Nan, G. L. and Walbot, V. (2009). Nonradioactive genomic DNA blots for detection of low abundant sequences in transgenic maize. *Methods Mol. Biol.* **526**, 113-122.
Nonomura, K., Miyoshi, K., Eiguchi, M., Suzuki, T., Miyao, A., Hirochika, H. and Kurata, N. (2003). The MSP1 gene is necessary to restrict the number of cells entering into male and female sporogenesis and to initiate anther wall formation in rice. *Plant Cell* **15**, 1728-1739.
Poethig, R. S. (1987). Clonal analysis of cell lineage patterns in plant development. *Am. J. Bot.* **74**, 581-594.
Rojo, E., Sharma, V. K., Kovaleva, V., Raikhel, N. V. and Fletcher, J. C. (2002). CLV3 is localized to the extracellular space, where it activates the Arabidopsis CLAVATA stem cell signaling pathway. *Plant Cell* **14**, 969-977.
Schiefthaler, U., Balasubramanian, S., Sieber, P., Chevalier, D., Wisman, E. and Schneitz, K. (1999). Molecular analysis of NOZZLE, a gene involved in pattern formation and early sporogenesis during sex organ development in Arabidopsis thaliana. *Proc. Natl. Acad. Sci. USA* **96**, 11664-11669.
Scott, A., Wyatt, S., Tsou, P.-L., Robertson, D. and Allen, N. S. (1999). Model system for plant cell biology: GFP imaging in living onion epidermal cells. *BioTechniques* **26**, 1125-1132.
Sharma, V. K., Ramirez, J. and Fletcher, J. C. (2003). The Arabidopsis CLV3-like (CLE) genes are expressed in diverse tissues and encode secreted proteins. *Plant Mol. Biol.* **51**, 415-425.
Sheridan, W. F., Avalkina, N. A., Shamrov, I. I., Batygina, T. B. and Golubovskaya, I. N. (1996). The mac1 gene: Controlling the commitment to the meiotic pathway in maize. *Genetics* **142**, 1009-1020.
Sheridan, W. F., Golubeva, E. A., Abrhamova, L. I. and Golubovskaya, I. N. (1999). The mac1 mutation alters the developmental fate of the hypodermal cells and their cellular progeny in the maize anther. *Genetics* **153**, 933-941.
Vernoud, V., Laigle, G., Rozier, F., Meeley, R. B., Perez, P. and Rogowsky, P. M. (2009). The HD-ZIP IV transcription factor OCL4 is necessary for trichome patterning and anther development in maize. *Plant J.* **59**, 883-894.
von Arnim, A. G., Deng, X. W. and Stacey, M. G. (1998). Cloning vectors for the expression of green fluorescent protein fusion proteins in transgenic plants. *Gene* **221**, 35-43.
Willmann, M. R. (2000). CLV1 and CLV3: negative regulators of SAM stem cell accumulation. *Trends Plant Sci.* **5**, 416.
Yang, S. L., Xie, L. F., Mao, H. Z., Puah, C. S., Yang, W. C., Jiang, L., Sundaresan, V. and Ye, D. (2003). Tapetum determinant1 is required for cell specialization in the Arabidopsis anther. *Plant Cell* **15**, 2792-2804.
Yang, S. L., Jiang, L., Puah, C. S., Xie, L. F., Zhang, X. Q., Chen, L. Q., Yang, W. C. and Ye, D. (2005). Overexpression of TAPETUM DETERMINANT1 alters the cell fates in the Arabidopsis carpel and tapetum via genetic interaction with excess microsporocytes1/extra sporogenous cells. *Plant Physiol.* **139**, 186-191.
Yang, W. C., Ye, D., Xu, J. and Sundaresan, V. (1999). The SPOROCYTELESS gene of Arabidopsis is required for initiation of sporogenesis and encodes a novel nuclear protein. *Genes Dev.* **13**, 2108-2117.
Zhao, S. and Fernald, R. D. (2005). Comprehensive algorithm for quantitative real-time polymerase chain reaction. *J. Comput. Biol.* **12**, 1047-1064.
Zhao, D. Z., Wang, G. F., Speal, B. and Ma, H. (2002). The excess microsporocytes1 gene encodes a putative leucine-rich repeat receptor protein kinase that controls somatic and reproductive cell fates in the Arabidopsis anther. *Genes Dev.* **16**, 2021-2031.
Zhao, X., de Palma, J., Oane, R., Gamuyao, R., Luo, M., Chaudhury, A., Herve, P., Xue, Q. and Bennett, J. (2008). OsTDL1A binds to the LRR domain of rice receptor kinase MSP1, and is required to limit sporocyte numbers. *Plant J.* **54**, 375-387.

Table S1. Primers used in this study

Name	Sequence	Notes*,‡
P229	GCCGGCAGCTGCGTGGTAGAGGAAC	1F
P228	GTTTCGCAGTAGGGTTTGGTGAGGGTGGTC	1R
P227	TGACCAGAAGCGGACAAGACCAGAAC	2F
P226	GATGGAGCGGCGACAAGGGAGGGAC	2R
P225	CCGCCTGGCTATACGAAACCGACTCTG	3F
P224	AATGGTGTTGGTGATCGAAGGTGGAAAAG	3R
P223	TATCCGGTTCCGTTGCTCCATTCTCGTA	4F
P222	CCCCCGCCCTCGCTTCGCTATC	4R
P221	GCGGCCCCATCCCCAGCACTGTTTTGTAT	5F
P220	GTGCGGACTGCGGACGGAGCGACAT	5R
P219	CCTGCGCCACGACGACTGCCTCCTCAAC	6F
P218	GCCCAAAAATTTCACATCCCGCATCCAGT	6R
P217	CTCCGCGTTTTGTTCTTTTGCCGATGTTC	7F
P216	AGTCACCCCCATCCCACCACCTCTGTC	7R
P238	CCGTGGTGCCTTGTTTGCTTGCTCGCTCA	8F
P239	GGGCACATCCAATACAATAATCCTCCATA	8R
P240	CGGCGGGCCCAAGATCGATTTTCCTATT	9F
P241	CCGTTCCGTTCGTGCCACCATCATTGTTA	9R
P242	TACGAAGAGCTGAAATCAAACACATAAT	10F
P243	CGTCCCGGTCGATCCTTCAAACAG	10R
P258	GCCTCCATTTCGTCGAATCC	Universal *Mu*TIR
P292	AGTATCTTGCGGGGCAGTG	R
F14	AACCCTACTGCGAAACAACTGC	F
R15	ATCAGGACGCAGGATTCTCG	R
cyanase	GCTGGTGAGGAGGAGAAACA	F
cyanase	CAGCAATCATGCCAGGTAGA	R

*The first ten pairs of primers (1F-10R) were first used to identify the deletion in the *mac1-1* mutant.

‡Primers P222, P223 and P220, P223 were used for *mac1-1* genotyping, and primers P222, P223, P258 and P292 for *mac1-Y211* genotyping.

Table S2. Independent segregation of *mac1* and *am1*

Crosses and families*	Segregation fertile:sterile‡	Cytology female meiosis in sterile plants§			Total¶
		mac1/mac1	*am1/am1*	*mac1/mac1 am1/am1*	
1. F2 (*am1-485*/+ × *mac1*+)	28:17	7	8	1	16
2. F2 (*am1-1*/+ × *mac1*/+)	28:17	7	3	3	13
3. F2 (*am1-2*/+ × *mac1*/+)	32:18	8	3	1	12
Total	88:52	22	14	5	41
χ^2	χ^2 (9:7) = 2.47			χ^2 (3:3:1) =2.56	

*The individual crosses started from the heterozygotes of two mutants (*mac1*/+ × *am1*/+). The F1 plants were self-pollinated and F2 were studied. This experiment was carried out before molecular cloning of the *am1* and *mac1* genes. All genotypes were determined by genetic crosses.

‡Only F2 families segregating fertile and sterile plants with the expected ratio 9:7 were further analyzed. Meiotic phenotypes of all fertile plants were verified with aceto-carmine squashes of young anthers to confirm their normal meiosis.

§The sterile plants in these families were further investigated. Several ovules of each sterile plant were squashed, and megaspore mother cells (MMC) were isolated. The number of MMCs and the meiosis status were studied as previously described (Sheridan et al., 1996). Plants with single MMC per ovule showing the mitotic *am1-1* phenotype were grouped in the *am1* mutant class. Plants with multiple MMCs and regular meiosis were grouped in the *mac1* mutant class. Double mutant *am1; mac1* ovules exhibited both phenotypes as they contained multiple MMCs that conducted the aberrant *am1* meiocyte mitosis. The expected ratio of these three classes is 3:3:1.

¶Total numbers of sterile plants investigated by microscopic evaluation. The total χ^2 values are shown in the last cell of the column.

Table S3. Independent segregation of *mac1* and *afd1*

Crosses and families*	Segregation fertile:sterile‡	Cytology female meiosis in sterile plants§			Total¶
		mac1/mac1	*afd1/afd1*	*mac1/mac1 afd1/afd1*	
1. F2 (*afd1-1/+* × *mac1+*)	31:32	12	17	3	32
2. F2 (*afd1-1/+* × *mac1+*)	40:35	18	14	3	35
Total	71:67	30	31	6	67
Expected if 9:3:3:1	77.6:60.4	25.9	25.9	8.6	
χ^2 (9:3:3:1)	0.56	0.52	1.01	0.8	2.39

*The individual crosses started from heterozygotes of two mutants (*mac1/+* × *afd1/+*). The F1 plants were self-pollinated and F2 were studied. This experiment was carried out before molecular cloning of the *afd1* and *mac1* genes; therefore, all genotypes were determined by genetic crosses.

‡Only F2 families segregating fertile and sterile plants with the expected ratio 9:7 were further analyzed. The meiotic phenotype of all fertile plants was screened using aceto-carmine squashes of young anthers to confirm their normal meiosis.

§The sterile plants in these families were further investigated. Several ovules of each sterile plant were squashed, and megaspore mother cells (MMC) were isolated, counted and scored for meiotic characteristics previously described (Sheridan et al., 1996). Plants with a single MMC per ovule showing the *afd1* meiotic phenotype were grouped in the *afd1* mutant class. Plants with multiple MMCs and regular meiosis were grouped in the *mac1* mutant class. Double mutants, *afd1; mac1*, expressed both phenotypes as they contained multiple MMCs with the *afd1* meiotic defect. The expected ratio of these three classes is 3:3:1.

‡Total number of sterile plants investigated microscopically. The total χ^2 values are shown in the last cell of the column.

Table S4. Numbers of ovules, megaspore mother cells analyzed in six *mac1/mac1; afd1/afd1* double mutant plants

Family	Numbers of ovule examined	Megaspore mother cells (MMCs)		Stages of meiosis						
		Average	Total	Inter-phase	L-P	Dia	M1-T1	Dyad	Triad	Tetrad
1-14	70	4.9 (2-9)	340	11	276	3	26	23	1	0
1-26	45	7.1 (3-14)	320	10	175	1	21	82	28	3
1-57	40	4.0 (2-8)	159	4	121	1	6	26	1	0
Subtotal	155	5.3 (2-14)	819	25	572	5	53	131	30	3
2-7	10	5.9 (4-10)	59	1	15	9	4	21	2	7
2-15	5	6.0 (4-7)	30	0	11	0	3	7	5	4
2-21	13	7.1 (4-10)	93	4	59	6	9	11	1	3
Subtotal	28	6.5 (4-10)	182	5	85	15	16	39	8	14
Total	**183**	**5.5 (2-14)**	**1001**	**30**	**657**	**20**	**69**	**170**	**38**	**17**

L-P, leptotene throughout oachytene; Dia, diakinesis; M1-T1, metaphase 1 throughout telophase 1.